ELSEVIER

Contents lists available at ScienceDirect

Colloids and Surfaces B: Biointerfaces

journal homepage: www.elsevier.com/locate/colsurfb





Characterization of size-tuneable aescin-lipid nanoparticles as platform for stabilization of membrane proteins

Fatima Escobedo ^{a,b}, Mohanraj Gospalswamy ^c, Pia Hägerbäumer ^d, Tim Julian Stank ^d, Julian Victor ^a, Georg Groth ^e, Holger Gohlke ^{c,f}, Carina Dargel ^{d,g,*}, Thomas Hellweg ^{d,**}, Manuel Etzkorn ^{a,b,***}

- a Heinrich Heine University Düsseldorf, Faculty of Mathematics and Natural Sciences, Institute of Physical Biology, Universitätsstr. 1, Düsseldorf 40225, Germany
- b Institute of Biological Information Processing (IBI-7: Structural Biochemistry), Forschungszentrum Jülich GmbH., Wilhelm-Johnen-Str, Jülich 52425, Germany
- ^c Heinrich Heine University Düsseldorf, Faculty of Mathematics and Natural Sciences, Institute for Pharmaceutical and Medicinal Chemistry, Universitätsstr. 1, Düsseldorf 40225, Germany
- ^d Physical and Biophysical Chemistry, Bielefeld University, Universitätsstr. 25, Bielefeld 33615, Germany
- ^e Heinrich Heine University Düsseldorf, Faculty of Mathematics and Natural Sciences, Institute for Biochemical Plant Physiology, Universitätsstr. 1, Düsseldorf 40225, Germany
- f Institute for Bio, and Geosciences (IBG-4: Bioinformatics), Forschungszentrum Jülich GmbH., Wilhelm-Johnen-Str, Jülich 52425, Germany
- g Institute of Physical Chemistry, University of Münster, Corrensstraße 28/30, Münster 48149, Germany

ARTICLE INFO

Keywords: nuclear magnetic resonance (NMR) aescin-DMPC-nanoparticles molecular interaction bacteriorhodopsin (BR)

ABSTRACT

Disc-like lipid nanoparticles stabilized by saponin biosurfactants display fascinating properties, including their temperature-driven re-organization. β -Aescin, a saponin from seed extract of the horse chestnut tree, shows strong interactions with lipid membranes and has gained interest due to its beneficial therapeutic implications as well as its ability to decompose continuous lipid membranes into size-tuneable discoidal nanoparticles. Here, we characterize lipid nanoparticles formed by aescin and the phospholipid 1,2-dimyristoyl-sn-glycero-3-phosphocholine. We present site-resolved insights into central molecular interactions and their modulations by temperature and aescin content. Using the membrane protein bacteriorhodopsin, we additionally demonstrate that, under defined conditions, aescin-lipid discs can accommodate medium-sized transmembrane proteins. Our data reveal the general capability of this fascinating system to generate size-tuneable aescin-lipid-protein particles, opening the road for further applications in biochemical, biophysical and structural studies.

1. Introduction

Aescin, also called escin, is an isomeric mixture of α - and β -triterpene saponins obtained from the extract of the seeds of the horse chestnut tree *Aesculus hippocastanum* [1–4]. It was reported that β -aescin has anti-inflammatory, anti-oedematous, and venotonic properties, as well as antifungal and antibacterial activity. Therefore, it has emerged as an active component in the treatment of heart failure, varicose veins, haemorrhoids, diarrhea, fever, cancer, and rheumatism [4–10]. Part of the biological activity of β -aescin may involve its interaction with biological membranes, which in turn is related to its molecular structure

comprising a hydrophilic head group composed of two glucose molecules and a glucuronic acid attached to a hydrophobic triterpenic backbone (see Fig. 1a) [7,11]. This amphiphilic structure leads to surface activity and formation of β -aescin micelles above a critical micelle concentration [11]. Moreover, its molecular structure is the reason for the interaction of aescin with lipid membranes, which, at low aescin content, induces a change of the membrane elasticity due to aescin incorporation into the lipid matrix [12]. With increasing aescin content this incorporation further leads to aggregation of either intact vesicles or large membrane fragments and ultimately to complete membrane solubilisation into disc-like nanoparticles [4,13–15]. Nanoparticle

E-mail addresses: cdargel@uni-muenster.de (C. Dargel), thomas.hellweg@uni-bielefeld.de (T. Hellweg), manuel.etzkorn@hhu.de (M. Etzkorn).

https://doi.org/10.1016/j.colsurfb.2024.114071

^{*} Corresponding author at: Institute of Physical Chemistry, University of Münster, Corrensstraße 28/30, Münster 48149, Germany.

^{**} Correspondence to: Physical and Biophysical Chemsitry, Bielefeld University, Universitätsstr. 25, 33615 Bielefeld, Germany.

^{***} Corresponding author at: Heinrich Heine University Düsseldorf, Faculty of Mathematics and Natural Sciences, Institute of Physical Biology, Universitätsstr. 1, Düsseldorf 40225, Germany.

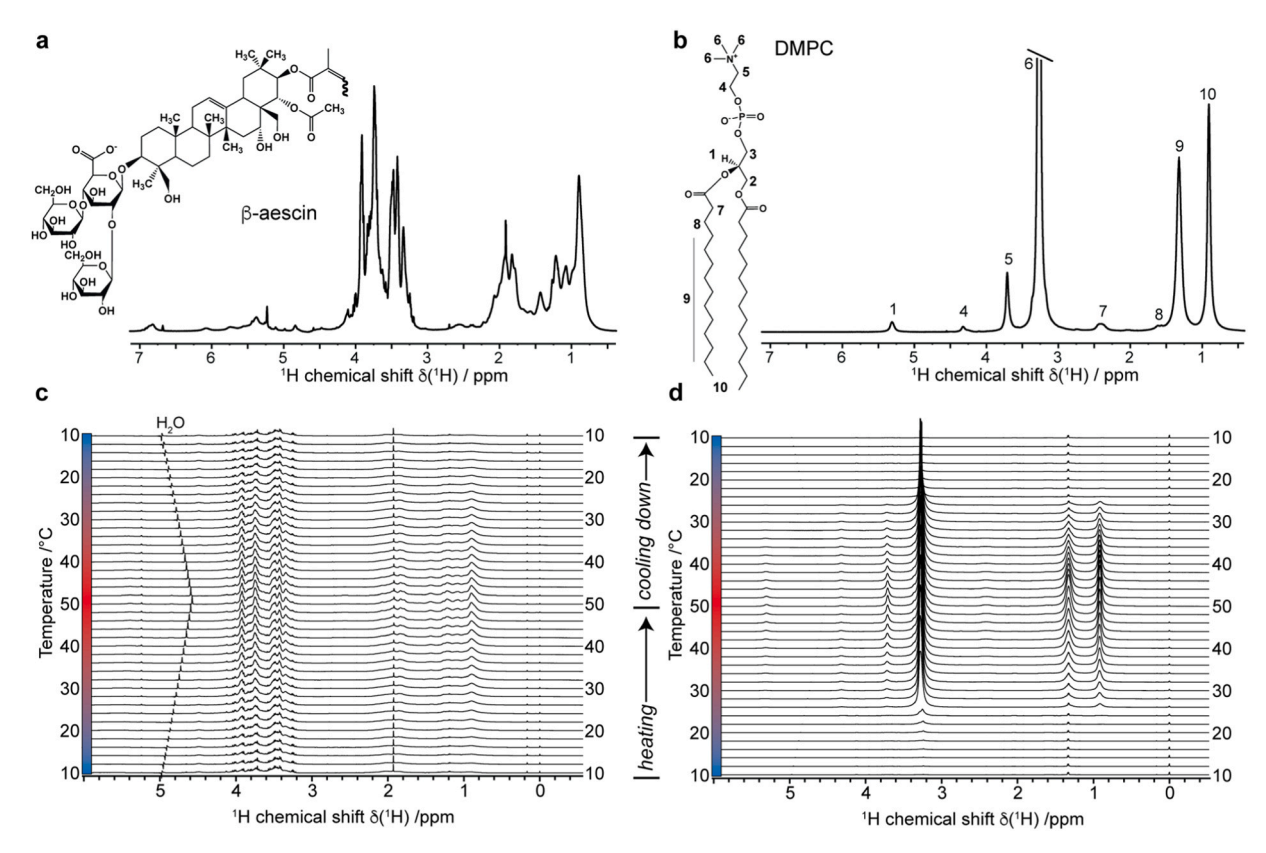


Fig. 1. ^{1}H NMR spectra and NMR-temperature profiles of individual components. a) Chemical structure of β -aescin and its NMR spectrum. b) Chemical structure and NMR spectrum of DMPC SUVs. Respective NMR resonance assignments are indicated for dominant peaks. NMR-temperature profiles of aescin (c) and DMPC SUVs (d) measured between 10 $^{\circ}$ C and 50 $^{\circ}$ C under stepwise increasing temperatures followed by stepwise decreasing temperatures. NMR spectra in a) and b) reflect respective spectra recorded at 40 $^{\circ}$ C (during the heating period).

formation of aescin with lipids has so far been investigated particularly with regard to the zwitterionic phospholipid 1,2-dimyristoyl-sn-glycero-3-phosphocholine (DMPC). In these particles, the hydrophobic outer edge of a circular-shaped DMPC membrane fragment is stabilized by a layer of amphipathic aescin molecules. The resulting discoidal lipid structures are known as bicelles or nanodiscs [12,16], which were not found for DMPC alone at the respective temperatures [14].

Previous NMR studies using bicelles formed with DMPC lipids and heterogeneous mixtures of saponins extracted from Quillaja Molina trees have provided initial insights into the effects of saponins on the lipids, and could further demonstrate that the system can be used to conveniently produce large bicelles that align in the magnetic field, enabling specific NMR-based readouts such as residual dipolar couplings [17]. For the more homogenous and better-defined β -aescin system, previous studies, predominantly using neutron, X-ray and light scattering, have also revealed that aescin-lipid particle shape, stability and size are correlated with the aescin:phospholipid ratio; likewise, it was found that the interaction of β-aescin with lipid bilayers is highly dependent on the lipid phase state and thus is temperature-dependent [4,12,14,15]. These characteristics make β -aescin a promising candidate for the stabilization of hydrophobic molecules, such as integral membrane proteins, within the lipid membrane. Furthermore, aescin-lipid particles might also be of interest in the context of drug delivery. While previous studies have used scattering methods to obtain detailed insights into structural parameters such as the global size and thickness of lipid and β -aescin layers [4,14, 15], information about the size-adaptation processes and the aescin-lipid interactions on a molecular level is sparse.

Here, we provide a NMR-based characterization of β -aescin-lipid mixtures and their complex temperature- and concentration-dependent interactions to better understand the system on a molecular level. Using bacteriorhodopsin (BR) as an established model system for

transmembrane proteins, we furthermore explore the possibilities of using aescin-DMPC discoidal nanoparticles as a membrane-mimicking environment. Our data demonstrate that aescin-DMPC discs are indeed well-capable of stabilizing BR, while maintaining their general features such as size-tunability and solubility; thus, highlighting the potential of this intriguing system as an alternative platform to stabilize membrane proteins.

2. Material & methods

2.1. Sample preparation

DMPC in chloroform stock (Avanti Polar Lipids. Inc (Alabaster, AL)) were dried under nitrogen flow to obtain a thin lipid film and subsequently stored under vacuum overnight for complete chloroform removal. Then, the dry film was hydrated by a previously prepared β-aescin solution at the desired β-aescin concentration dissolved in 50 mM phosphate buffer at pH 7.4. All prepared samples had the final DMPC mass concentration of w(DMPC) = 15 g/L, while the β-aescin content ranges from 0 to 30 mol% with respect to DMPC. The saponin β-aescin was obtained from Sigma Aldrich (>95 %, CAS-number 6805–41–0, Munich, Germany). The samples were exposed to five freeze-thaw cycles in liquid nitrogen and warm water (well above $T_{m, \text{DMPC}} \approx 24 \,^{\circ}\text{C}$). DMPC small unilamellar vesicles (SUVs) were prepared by extrusion through 100 nm pore diameter membranes (Avanti Polar Lipids, Inc.) at 35 $\,^{\circ}\text{C}$ and the aescin-DMPC bicelles were formed by self-assembly when the β -aescin content exceeds 7 mol%.

2.2. Dynamic light scattering

The bicelles' hydrodynamic diameters were analysed by dynamic

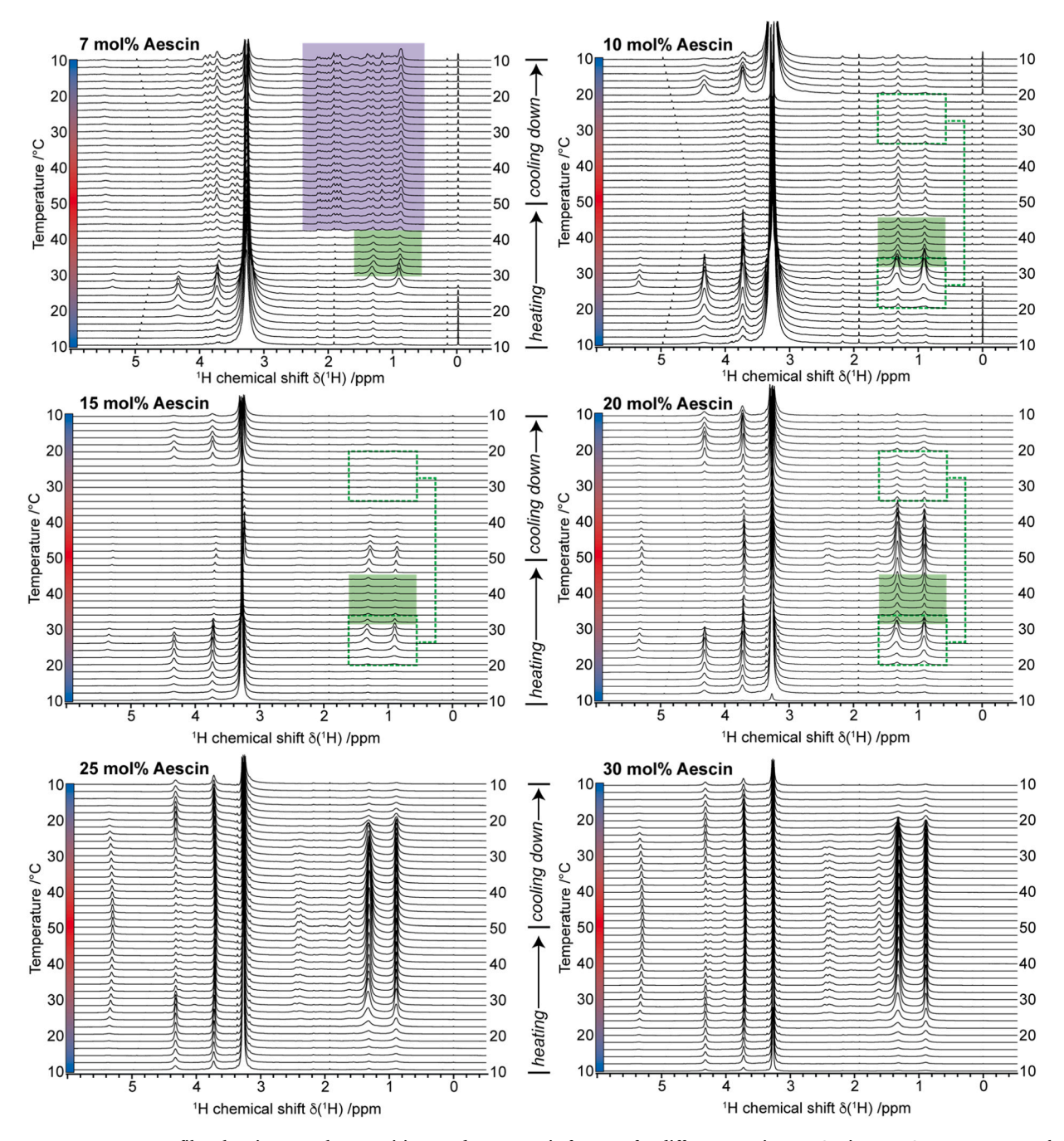


Fig. 2. NMR-temperature profiles showing complex transitions and asymmetric features for different aescin-DMPC mixtures. Spectra were recorded as in Fig. 1c,d, but using aescin-DMPC mixtures at indicated molar fractions of aescin. Selected features are highlighted with different colours including the occurrence of a distinct state only present at 7 mol% aescin (purple area), (exchange) processes leading to signal intensity losses (green areas), and asymmetric features indicative of energetically trapped states (dotted green lines, see text for more details).

light scattering (DLS) using a Zetasizer Nano-ZS device (Malvern Systems, Worcestershire, UK) equipped with a laser source of wavelength $\lambda=633$ nm. All samples were measured in 10 mm diameter polystyrene cuvettes at 25 °C. The number-average diameter results were obtained and processed in Zetasizer Software v8.02. All samples were centrifuged for 25 min at 12500x g prior to measurements to remove precipitates. Aescin-DMPC-BR particles assembled at a ratio of 7 mol% β -aescin showed noticeable turbidity even after centrifugation rendering DLS data for this ratio less reliable.

2.3. NMR analysis

All 1D and 2D 1 H spectra were recorded on a 600 MHz Bruker Avance III HD $^+$ spectrometer. All nanoparticle samples were measured in the same buffer (50 mM sodium phosphate pH 7.4 90 % H₂O/10 % D₂O). 1D spectra were recorded in a temperature range from 10 $^{\circ}$ C to 50 $^{\circ}$ C with two-degree increments and continuous NMR acquisitions with a duration of approx. 2.5 min for each temperature step. 2D NOESY spectra were recorded with 128 scans at 10 $^{\circ}$ C and 40 $^{\circ}$ C. All peaks were assigned by comparing with previous assignments and the Spectral Database for Organic Compounds for DMPC and β -aescin. All NMR data were processed using the TopSpin 3.5 software (Bruker) and analysed

using Sparky [18].

The DMPC's ¹H chemical shift perturbation (CSP) values were calculated as the difference from the respective frequency in the absence of aescin and otherwise identical experimental conditions.

2.4. Bacterioopsin expression

The protein bacterioopsin (BO) was expressed as a fusion construct inserted into the expression vector pIVEX2.4d. The fusion construct of BO comprises a 10x N-terminal His tag, a factor Xa cleavage site, and the BO sequence. The BO cell-free protein expression was carried out using an $E.\ coli$ -based system following published procedures [19,20]. The resulting protein pellet was washed with S30 buffer to remove impurities and either directly refolded or stored at $-20\ ^{\circ}$ C.

2.5. Folding and incorporation of bacteriorhodopsin (BR) into aescin-DMPC particles

The refolding of BO into n-dodecyl- β -D-maltoside (DDM) micelles was performed following published protocols [20]. In short, the washed protein pellet was resuspended with DDM-refolding buffer, which consisted of 50 mM sodium phosphate (pH 7), 1 M NaCl, 5 % (w/v) DDM, and 100 μ M retinal. Refolding of BO in presence of retinal leads to formation of intact bacteriorhodopsin (BR) as validated by a characteristic colour change of the sample within minutes. The refolded BR-DDM micelles were then combined with a previously prepared aescin-DMPC mixture at the desired concentration of β -aescin.

The removal of DDM was performed using two strategies. In the first setup, we carried out a stepwise buffer exchange to substitute DDM micelles by centrifugal filters (20 kDa cutoff). After the sample volume of BR-DDM was reduced from 10 ml to 0.5 ml, DDM-free aescin-DMPC buffer was added and the procedure was repeated 6-times. In the second setup, we used Ni-NTA agarose beads to remove DDM from immobilized BR, which enabled better control of the level of empty aescin-DMPC particles. 200 µL of BR (with 10xHis-tag) in DDM micelles at a concentration of 50 µM was incubated with 0.3 ml of the Ni-NTA agarose beads for 30 min. Subsequently, the sample was washed 5 times with one column volume of transfer buffer (50 mM NaPi pH 7.4, 20 mM imidazole) containing the respective concentrations of β -aescin and DMPC. The sample was eluted using 3 column volumes of elution buffer (50 mM NaP_i pH 7.4, 300 mM imidazole). For each aescin:DMPC ratio, two different elution protocols were applied using an elution buffer that was either supplemented with the same aescin-DMPC concentrations or did not contain additional aescin-DMPC. Visual inspection of all included preparations showed clearly visible purple colour after DDM removal, characteristic of folded BR.

3. Results

3.1. Characterization of aescin-DMPC particles

For our study, we focused exclusively on β -aescin, whose structural composition was clarified before [11]. For simplicity, we refer to this variant in the following as "aescin". To obtain site-resolved insights into the aescin-lipid interaction within the nanoparticle structures we carried out a set of NMR experiments. Initially, we recorded 1D 1H spectra of the individual components, i.e., buffer solubilized aescin (Fig. 1a,c) and DMPC prepared in the form of SUVs (Fig. 1b,d). Albeit partly overlapping peaks of DMPC and aescin complicate data analysis, distinguishable peaks between aescin and DMPC also enable NMR-based analysis of aescin-DMPC mixtures with molecule-specific resolution (see Fig. S1 for more details).

Previous studies revealed that aescin-DMPC interactions are strongly influenced by the respective molar ratios as well as by temperature effects [4,14,15]. Using a constant DMPC mass concentration of 15 g/L, it has been reported that aescin contents in the range between 10-30 mol

% (surpassing the critical micelle concentration of aescin) are particularly successful in forming monodisperse aescin-DMPC particles, while 7 mol% aescin represents a condition at the border between formation of bicelles and (aggregated) larger membrane fragments [12,15].

To investigate the temperature effects in more detail, we recorded a series of ¹H NMR spectra with increasing temperatures from 10 °C to 50 °C. Temperatures were initially increased in steps of 2 °C, followed by decreasing temperatures after reaching 50 °C. In general, increasing temperatures will lead to an increased molecular tumbling resulting in increased NMR intensities. Similarly, the temperature-induced transition of an ordered $L_{a'}$ -conformation into a more fluid L_{α} -phase, as present for the DMPC lipid-phase transition occurring at \approx 24 °C, will lead to an (additional) increase in the detected ¹H signal intensity. Noteworthy, the phase transition temperature of the DMPC lipids is increased by approx. 4 °C in the presence of the applied aescin concentrations, which should be considered when using the system [21]. First, temperature-dependent reference spectra of the respective isolated compounds were recorded (Fig. 1c,d). The data show that the NMR spectrum of aescin is only slightly affected by temperature (Fig. 1c). The most pronounced effect is a moderate broadening of the NMR signals at higher temperatures indicative of conformational exchange processes in the us to ms regime, which is in line with the previously observed transition from cylindrical to elliptical micelles [11]. As expected, the respective data for DMPC SUVs show a stronger temperature dependence (Fig. 1d). The observed behaviour is in line with a strong increase in peak intensities due to a more fluid lipid matrix after the gel-to-fluid phase transition of the DMPC bilayer. Noteworthy, for both isolated compounds the heating and cooling periods have very similar effects resulting in a symmetric appearance of the shown data.

Subsequently, we recorded a set of NMR spectra in the temperature regime between 10 and 50 °C as well as at aescin:DMPC molar ratios spanning from 7 – 30 mol% aescin at constant concentration of DMPC (22.15 mM, i.e., 15 g/L). The data reveal a complex behaviour of the mixtures that is not only strongly dependent on the applied temperature but also varies considerably with the molar ratio of aescin:DMPC (Fig. 2). In general, as also concluded from prior scattering data, the structural reorganization appears completely reversible for samples containing aescin contents above 10 mol% aescin. For the sample containing 7 mol% aescin, located at the border between bicelle and lipid sheet formation, this does not seem to be the case.

One notable feature of the different temperature profiles is a species with a distinct spectral appearance only found at 7 mol% aescin after the sample was heated up to above 44 °C (Fig. 2, 7 mol% aescin, purple area). Noteworthy, this state remains the dominant species even after the temperature is lowered well below the initial transition temperature, inducing highly asymmetric features in the temperature profile that report the occurrence of an energetically trapped state. The NMR signals of this state neither show obvious overlap with the NMR-characteristics of aescin nor of DMPC. In addition, the phase transition effects of the DMPC matrix, which are well observable during the heating period, are not observed during the cooling down period. The data highlight an additional temperature-induced transition above 42 °C that considerably and, on the detected time-scale, irreversibly modifies the properties of aescin-DMPC particles. While other explanations are possible, this behaviour would be well in line with a perturbation of the DMPC matrix by aescin molecules and a temperature-induced rearrangement into stacked membrane layers as reported before [12,14].

Besides full reversibility, an additional feature is found in the temperature profiles of the samples with 10-20 mol% aescin. These samples experience a prominent drop of the DMPC's NMR signals with increasing temperature in the range between $30-40\,^{\circ}\text{C}$, i.e., after the lipid phase transition (Fig. 2, filled green areas). In general, it would be expected that the NMR intensities of the respective peaks increase with temperature, as also seen for the pure DMPC sample (Fig. 1d). The observed decreasing NMR intensity would be in line with chemical exchange processes induced by fast fluctuations of aescin in the DMPC

a

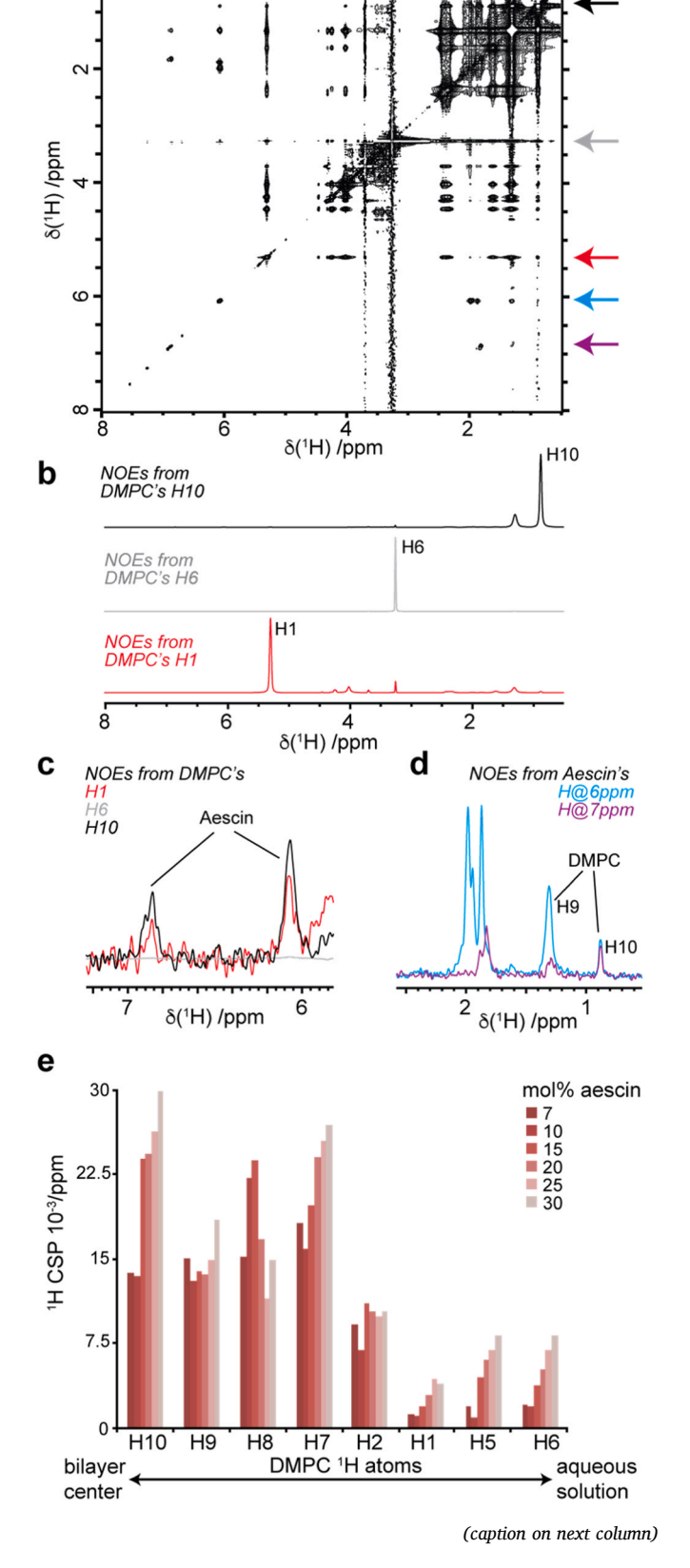


Fig. 3. Site-specific insights into aescin's interactions with DMPC show intermolecular contacts and a gradual increase from the DMPC's membrane interior to the solvent-exposed head groups. a) 2D $^{1}H^{-1}H$ NOESY spectrum of aescin-DMPC particles (30 mol% aescin, 40 $^{\circ}$ C) showing clear intermolecular contacts between aescin and DMPC. b) 1D slices extracted from spectrum in a) showing NOE correlations from the indicated spin to nearby ^{1}H atoms. Extraction frequencies are indicated by matching arrows in a) and autocorrelation (diagonal) peak is labelled. c) Spectral overlay and magnification of an aescin-specific region of spectra shown in b). d) Spectral overlay and magnification of spectral extract from a) corresponding to the indicated aescin ^{1}H spins. Note that in b-d) only the dominant spin of potentially overlapping frequencies is labelled. e) CSPs induced on DMPC by increasing concentrations of aescin. The DMPC's ^{1}H atoms are sorted according to their position along the membrane orthogonal.

matrix as well as with a temperature-induced increase in particle size. The latter would be consistent with temperature-induced fusion of the mixed nanoparticles that has also been observed via SAXS [14]. Noteworthy, the observed process also introduces an asymmetry in the temperature profiles, as for example seen by considerably reduced phase transition effects in the cooling down period (Fig. 2, green dotted areas, in the heating and cooling periods). This observation would also be in line with a mixing of aescin and DMPC leading to reduced cooperative effects in the DMPC bilayer during phase transition. In this view a fast incorporation of aescin into the DMPC matrix would be initially promoted by increasing temperatures and a more fluid bilayer, which in the cooling down period will only slowly release the incorporated aescin, trapping a fraction of the aescin molecules in the bilayer.

Looking at the behaviour of the samples with higher molar percentages of aescin (i.e., 25 mol% and 30 mol%) the data show a symmetric appearance indicative of a single state or interconvertible states with low energy barriers. Our data indicate that the temperature-induced size-variations observed via scattering methods for these "high-aescin" particles (25–30 mol% aescin) [14] are driven by fast processes such as rearrangements of the rim and/or dissolved aescin molecules within individual bicelles, while at lower aescin content slower processes such as the reassembly of molecules between different bicelles is more pronounced causing the asymmetric features in the NMR temperature profiles.

3.2. Mixing behaviour of aescin with the DMPC

To better characterize the molecular interactions between aescin and DMPC molecules we recorded a set of 2D NOESY spectra. These spectra allow the detection of close intermolecular contacts in the range between approx. 1-7 Å, referred to as nuclear Overhauser effect (NOE) contacts. Due to considerable signal overlap in larger spectral regions, it is not possible to derive an exact binding mode between the aescin and DMPC. However, distinct NOE contacts can still be identified confirming direct interactions of aescin with the lipid.

A cross-section through the 2D NOESY spectrum at the frequency of the DMPC's H10 (Fig. 3a, black arrow; Fig. 3b, black), reveals NOE contacts with at least two distinct aescin ¹H spins (Fig. 3c, black). Similarly, the cross-section at the frequency of DMPC's H1 (Fig. 3a, red arrow; Fig. 3b, red), shows a comparable pattern (Fig. 3c, red). Noteworthy, the spectral comparisons in Figs. 3b and 3c were scaled to match autocorrelation (diagonal) peak intensities. Consequently, the shown relative peak intensities of the NOE contacts allow an initial estimate of the strength of the interaction (reporting on different distances and/or populations). In this respect, the data suggest that DMPC's H10 shows a stronger interaction with aescin as compared to H1. By contrast, our data do not show interactions of DMPC's H6 with aescin (Fig. 3a-c, grey). Looking at the extracted cross-sections from the respective aescinspecific frequencies (Fig. 3a, blue and purple), the matching NOE contacts with the DMPC's H10 are found (Fig. 3d). Interestingly, the two aescin ¹H atoms show considerably different intermolecular NOE

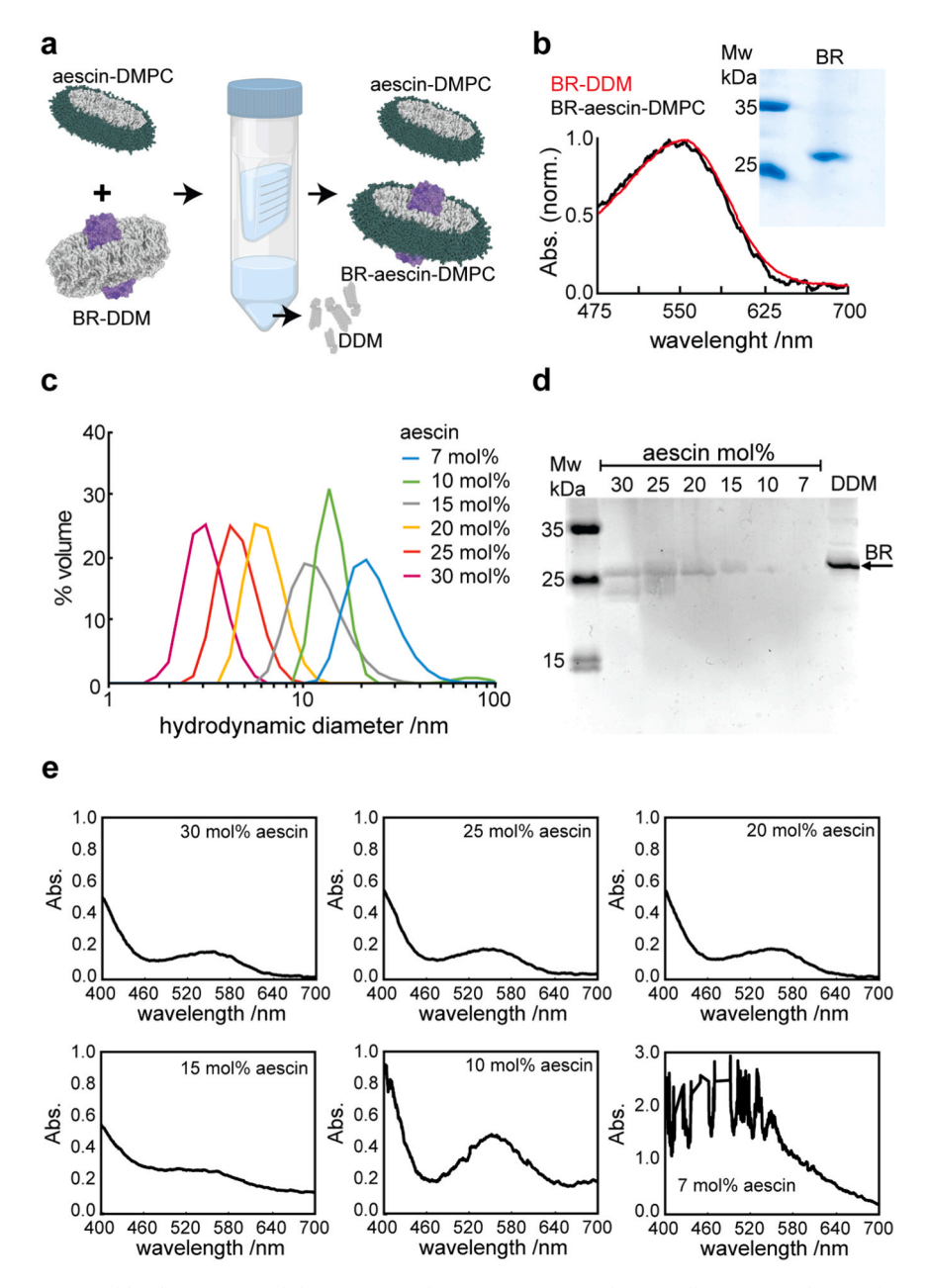


Fig. 4. Aescin-DMPC discs are a suitable platform to stabilize transmembrane proteins. a) Schematic illustration of the transfer of BR from DDM micelles into aescin-DMPC discs using centrifugal filters. b) Normalized absorption spectrum of BR before (red) and after transfer from DDM micelles into aescin-DMPC particles (25 mol% aescin, black). The absorption peak at 550 nm confirms the presence of folded BR. The inset shows SDS PAGE results of the DDM-refolded BR used as starting material. Effective removal of DDM after the transfer into aescin-DMPC discs was validated by NMR (Fig. S2). c) DLS data of resulting particles using indicated aescin:DMPC ratios. d) SDS PAGE analysis after transfer of BR into aescin-DMPC discs using the indicated different molar ratios of aescin. Only the soluble fractions after centrifugation are shown. An increasing yield of soluble BR-containing aescin-DMPC particles is observed with increasing content of aescin. e) Absorption spectra of BR in respective aescin-DMPC particles.

pattern indicative of a rather defined orientation of the aescin in respect to the hydrophobic part of the DMPC bilayer. Overall, the observed NOE correlations would be in line with a rather defined aescin belt formation in which the aescin shows the weakest contacts to the solvent-exposed DMPC ends (H6) and orients in a preferred orientation to the hydrophobic region of the lipids (H9, H10).

Complementary to the detection of direct intermolecular NOE contacts, chemical shift perturbations (CSPs) induced by changes in the molecular environment can be used as probes of molecular interactions. For example, replacing DMPC-DMPC packing with aescin-DMPC interactions will lead to changes in the resonance frequency of the spins that experience a different neighbour. Fig. 3e shows the CSPs induced in

different positions of the DMPC molecules by increasing concentrations of aescin. The data corroborate distinct effects of the presence of aescin on the different parts of the DMPC lipids. In this regard two features are visible, i.e. (i) the spins towards the membrane interior experience considerably stronger CSPs than the ones in the lipid head group, especially at lower aescin concentrations, and (ii) increasing the aescin concentration also has a clear effect on the head group's CSPs. These observations are in line with a preferential interaction of the aescin with the lipid's hydrocarbon chains, as for example present during belt formation as well as mixing, and a lower affinity interaction with the lipid's head groups that may become more relevant for increasing DMPC-aescin interfaces present in smaller discs that are expected at higher molar

 Table 1

 Particle sizes of different BR-aescin-DMPC preparations.

mol% aescin	hydrodynamic diameter / nm (via DLS)			
	Prep 1: Centrifugal filter ^a	Prep 2: On-column (w/ aescin) ^b	Prep 3: On-column (w/o aescin) ^c	Prep 4: Prep 3 + aescin- DMPC ^d
7	(19.6) ^e	(24.2) ^e	(18.4) ^e	-
10	13.5	13.5	21.0	12.5
15	6.9	10.8	23.1	12.2
20	5.6	10.8	18.0	11.2
25	4.2	11.9	15.6	8.6
30	3.6	8.1	10.6	8.3

^a DDM was removed via centrifugal filter (s. Fig. 4a).

ratios of aescin.

Overall, our data confirm the attractive properties of the aescin-DMPC system to tune the formation of distinct lipid-containing particles via temperature and/or varying the aescin:lipid ratio and may help to better understand the underlying mechanism and identify most suitable conditions for various applications.

3.3. Using aescin-DMPC nanoparticles as a platform to stabilize transmembrane proteins

One promising application of the aescin-lipid system is its potential capability to stabilize integral membrane proteins in size-tuneable particles. However, so far, no successful incorporation of a transmembrane protein into aescin-lipid particles has been reported. Therefore, we set

out to investigate the potential of the nanoparticles as membrane-mimicking environment using the established test protein bacteriorhodopsin (BR). BR contains seven transmembrane helices and its retinal cofactor exhibits a characteristic absorbance spectrum that can serve as a sensor of the BR's 3-dimensional structure [20,22,23]. In general, BR is known for its high stability and tolerance of different environments [20, 23,24], and paired with its directly accessible sensor of 3D structure, provides an excellent test system to assess whether medium-sized transmembrane proteins can be incorporated in aescin-lipid nanoparticles with intact 3D structure.

Following our previous strategies, cofactor-free bacterioopsin (BO) was expressed in a cell-free setup to ensure that no coordinated lipids would be transferred from the expressing organism [20,25]. The resulting BO pellet was simultaneously solubilized and refolded using retinal and DDM micelles containing buffer.

We applied two strategies to transfer the BR from DDM into aescin-DMPC particles. In a first setup, we carried out a stepwise buffer exchange to substitute DDM micelles via centrifugal filters (20 kDa cut-off) by adding (DDM-free) aescin-DMPC buffer (Fig. 4a). The resulting sample still contains soluble BR that exhibits the characteristic absorption spectrum (Fig. 4b). While ¹H NMR analysis shows that DDM has been effectively removed by this procedure (Fig. S2), the absorbance spectrum is identical to the one obtained in DDM (Fig. 4b, red), confirming that the BR structure is effectively maintained in the aescin-DMPC discs.

Due to the above-characterized importance of the applied aescin: DMPC ratios, we next varied this central parameter to evaluate the resulting capability to support protein solubilization and integrity as well as to assess the overall particle sizes of the respective aescin-DMPC-protein mixtures. For the latter DLS was used to determine the hydrodynamic diameter. As expected, the particle size decreases with increasing aescin content (Fig. 4c, Table 1), which coincides with the size dependence of the pure aescin-DMPC particles [15].

While here the initial DMPC concentration was kept constant at 15 g/L to enable a direct comparison with previously obtained scattering data [14,15], it should be noted that variations in DMPC

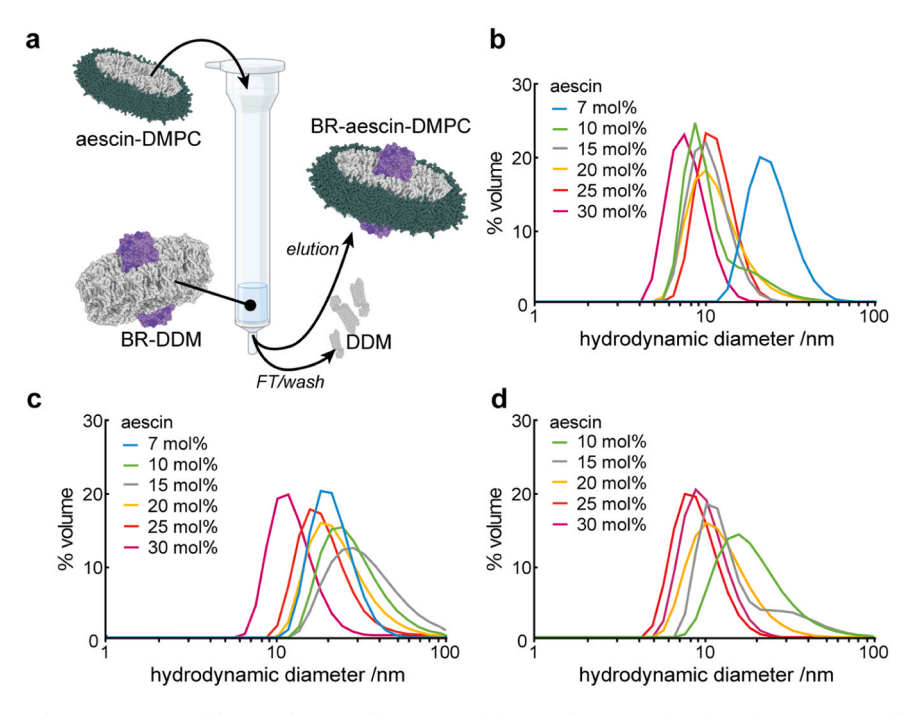


Fig. 5. BR-aescin-DMPC particles are size-tuneable. a) Schematic illustration of the on-column transfer of BR from DDM micelles into aescin-DMPC discs of different sizes. b-d) DLS profiles of resulting particles using different aescin:DMPC ratios and preparations. b) DLS data of samples prepared with indicated aescin amount in the transfer and elution buffer. c) DLS data of samples prepared with indicated aescin:DMPC ratios in the transfer buffer and using elution buffer not containing aescin-DMPC. d) DLS data of samples shown in c) after addition of empty aescin-DMPC discs prepared with the same aescin:DMPC ratios.

^b DDM was removed on Ni-NTA column (s. Fig. 5a) and eluted with buffer containing respective aescin-DMPC concentrations.

 $^{^{\}rm c}\,$ DDM was removed on Ni-NTA column and eluted with buffer containing no additional aescin-DMPC.

 $^{^{\}rm d}$ Samples from prep 3 were supplemented with defined aescin-DMPC levels after elution from Ni-NTA column.

 $^{^{\}rm e}$ Aescin-DMPC-BR particles assembled at ratios of 7 mol% aescin showed noticeable turbidity rendering DLS data less reliable.

concentrations may impact the formation and geometric features of aescin-lipid particles, similar to systems composed of zwitterionic lipids and different detergents [26]. In particular, when using low molar ratios of aescin (e.g., 7 mol%), lowering the DMPC concentration may lead to increased particle sizes and aggregation effects. Similarly, dilution of aescin-DMPC particles may induce particle rearrangements and aggregation. When using higher DMPC concentrations or when concentrating preformed aescin-DMPC particles dynamic rearrangements of the system may also be induced. These effects should be considered when using the system; particularly, when low molar ratios of aescin are present or when proteins are incorporated.

Our polyacrylamide gel electrophoresis (PAGE) data reveal increased BR content for samples with higher aescin concentrations, suggesting that successful BR incorporation into soluble aescin-DMPC particles is facilitated by higher aescin ratios (Fig. 4d). Note that the soluble fractions after centrifugation (15 min at 12.500x g) are shown. Absorbance spectra show that functional BR is found for all ratios; excluding 7 mol% aescin, which did not enable detection due to increased level of precipitation and low solubility (Fig. 4e). More quantitative analysis of PAGE and absorbance data, and including data recorded also at 50 mol% aescin, suggest that BR incorporation yield is best in the range between 15 and 30 mol% aescin with strongly reduced yields at or below 10 mol% and at or above 50 mol% aescin (see Supplementary Figure S3 for details). While the applied sample preparation method appears to be successful for most tested conditions, it generally affects the effective aescin:DMPC ratio in the resulting sample due to the different and not fully deductible effects of the centrifugal filter membrane on the dynamic exchange of the aescin-DMPC particles. In addition, the preparation will lead to large access of empty (i.e., not BRcontaining) particles perturbing the DLS data.

We therefore applied a second procedure to transfer BR from DDM micelles into aescin-lipid discs. We immobilized the BR in DDM micelles on Ni-NTA agarose beads to enable a more accurate exchange of the applied conditions and not accumulate empty bicelles (Fig. 5a). In a first set we eluted the BR-aescin-DMPC particles with buffer containing the same concentrations of aescin and DMPC as used during the BR transfer step (Fig. 5b). The resulting particles show increased sizes as compared to the same mixtures used with a centrifugal filter setup (Table 1, prep 2). Since the on-column method should provide better-defined sample conditions, the resulting sizes are expected to be more representative for the corresponding input conditions. Still, the used elution buffer contains also a considerable fraction of not-BR-containing particles, which may lead to averaging effects in the DLS measurements. We therefore repeated the same procedure but using an elution buffer without aescin or DMPC. The resulting particles show a further increased particle size (Fig. 5c, Table 1, prep 3). This observation can be explained either by predominantly isolating only BR-containing discs and/or by reassembly of the aescin-lipid particles due to reduction of the total aescin concentration.

To test a possible reassembly of BR-aescin-lipid particles, we added 4-fold excess of empty aescin-lipid particles to the respective preparations. DLS analysis shows a noticeable decrease in particle size for all tested conditions, indicating either a rearrangement of the particles or an averaging effect of the DLS measurement between empty and BR-containing discs (Fig. 5d, Table 1, prep 4).

Overall, our data demonstrate that nearly all tested conditions allow production of BR-aescin-DMPC particles that can effectively stabilize the transmembrane protein BR and point to convenient ways to tune the size of the aescin-lipid-protein particles. It should be stated that the term 'stabilized' is used here to illustrate the formation of a stable, i.e., intact protein structure. In comparison to other membrane-mimicking systems, we anticipate that the thermal stability is not necessarily increased due to the inherent dynamic nature of the aescin-DMPC system. However, experimental characterizations of the thermal stability are limited by the hydrophobic feature of the aescin system interfering with thermoflour assays and the absorbance of aescin at 280 nm (Fig. S3a) interfering with

intrinsic fluorescence detection.

While here our aim was to demonstrate the general feasibility to use aescin-lipid particles as membrane mimetics and it is too early to evaluate the full advantages of the aescin-lipid particles as new general platform for membrane protein stabilization, we speculate that inherent favorable features of the system include: (i) direct availability of large aescin quantities at low costs and without need for protein/peptide production or purification, (ii) as food extract (from the chestnut), its usage in therapeutic applications is facilitated, and (iii) it offers convenient ways to adjust particle size and shape. Unfavorable features will include a limited thermal stability and heterogeneities associated with the heterogenous aescin extracts.

4. Conclusion

Our data provide new insights into the interaction of the saponin aescin and the phospholipid DMPC when present in the form of mixed nanoparticles on a molecular level and thus significantly expand the structural view that was previously obtained exclusively from scattering experiments. The observed strong dependence of aescin-DMPC mixing and disc formation on the temperature and aescin:DMPC ratio is generally well in line with the previous scattering results. An unexpectedly large number of NMR-spectroscopic distinct states could be discovered. In particular, our data show a general reversibility of the temperature-dependent structural reorganization in a wide range of aescin contents (10 - 30 mol%). However, only at very high aescin content (≥ 25 mol%) the transition occurs without hysteresis effects. This observation suggests that at very high aescin contents slower processes such as inter-particle rearrangements are less pronounced, whereas at lower aescin contents inter-particle interactions (fusion, disintegration and/or resorting) may constitute a rate-limiting process in size-adaptation. This effect also leads to an energetically trapped state at very low aescin contents (7 mol%). In addition, we showed that structure formation in aescin-DMPC mixtures is mainly controlled by interactions with the hydrophobic part of the lipid, pointing to a plausible entropy-driven link between temperature-dependence and structure formation. Moreover, our data reveal that aescin-lipid particles allow to stabilize transmembrane proteins while still maintaining their intriguing properties of changing the particle size by changing the aescin:lipid ratio. This may open up exciting new avenues of the aescin system as a size-tuneable platform for future structural and functional studies of (trans-)membrane proteins.

CRediT authorship contribution statement

Manuel Etzkorn: Writing – original draft, Visualization, Supervision, Methodology, Funding acquisition, Formal analysis, Conceptualization. Fatima Escobedo: Writing – original draft, Validation, Investigation, Formal analysis, Conceptualization. Mohanraj Gospalswamy: Investigation, Formal analysis. Pia Hägerbäumer: Methodology, Investigation, Writing – original draft. Tim Julian Stank: Writing – original draft, Investigation, Formal analysis. Julian Victor: Investigation, Formal analysis. Georg Groth: Supervision, Funding acquisition. Holger Gohlke: Writing – original draft, Supervision, Funding acquisition. Carina Dargel: Writing – original draft, Visualization, Supervision, Formal analysis, Conceptualization. Thomas Hellweg: Writing – original draft, Supervision, Funding acquisition, Conceptualization.

Declaration of Competing Interest

The authors declare that they have no known competing financial interests or personal relationships that could have appeared to influence the work reported in this paper.

Data availability

Data will be made available on request.

Acknowledgements

The authors acknowledge access to the Jülich-Düsseldorf Biomolecular NMR Center. This work was supported by the German Research Foundation (DFG) (ET 103/4–1, ET 103/4–3, and the Heisenberg grant ET 103/5–1) to M.E. and (HE 2995/7–1) to T.H.

Appendix A. Supporting information

Supplementary data associated with this article can be found in the online version at doi:10.1016/j.colsurfb.2024.114071.

References

- [1] V.R. Netala, S.B. Ghosh, P. Bobbu, D. Anitha, V. Tartte, Triterpenoid saponins: a review on biosynthesis, Applications and mechanism of their action, Int J. Pharm. Pharm. Sci. 7 (2015) 24–28.
- [2] J.A. Wilkinson, A.M.G. Brown, Horse chestnut Aesculus hippocastanum: potential applications in cosmetic skin-care products, Int J. Cosmet. Sci. 21 (1999) 437–447.
- [3] A. Costantini, Escin in pharmaceutical oral dosage forms: quantitative densitometric HPTLC determination, Farmaco 54 (1999) 728–732.
- [4] R. Geisler, C. Dargel, T. Hellweg, The biosurfactant β-aescin: a review on the physico-chemical properties and its interaction with lipid model membranes and langmuir monolayers, Molecules 25 (2020) 1–22.
- [5] E.E. Pittler MH, Horse chestnut seed extract for venous insufficiency. Alternative Therapies in, Women's. Health 9 (2007) 25–27.
- [6] M. Dudek-Makuch, E. Studzińska-Sroka, Horse Chestnut efficacy and safety in chronic venous insufficiency: an overview. Revista Brasileira de, Farmacognosia 25 (2015) 533–541.
- [7] C.R. Sirtori, Aescin: pharmacology, pharmacokinetics and therapeutic profile, Pharm. Res. 44 (2001) 183–193.
- [8] L. Gallelli, Escin: a review of its anti-edematous, anti-inflammatory, and venotonic properties, Drug Des. Devel Ther. Volume 13 (2019) 3425–3437.
- [9] E. Harford-Wright, N. Bidère, J. Gavard, β-escin selectively targets the glioblastoma-initiating cell population and reduces cell viability, Oncotarget 7 (2016) 66865.

- [10] A. Vasiliauskas, L. LeonaviĈienė, D. Vaitkienė, R. Bradūnaitė, A. Lukšienė, Antiinflammatory effects of Aesculus hippocastanum L. tincture and the pro-/ antioxidant bodily state of rats with adjuvant arthritis, Acta Medica Lituanica 17 (3) (2010) 123–132.
- [11] C. Dargel, et al., Self-assembly of the bio-surfactant aescin in solution: a small-angle x-ray scattering and fluorescence study, Colloids Interfaces 3 (2019) 47.
- [12] R. Sreij, et al., Temperature dependent self-organization of DMPC membranes promoted by intermediate amounts of the saponin aescin, Biochim Biophys. Acta Biomembr. 1861 (2019) 897–906.
- [13] R. Sreij, C. Dargel, L.H. Moleiro, F. Monroy, T. Hellweg, Aescin incorporation and nanodomain formation in DMPC model membranes, Langmuir 33 (2017) 12351–12361.
- [14] R. Geisler, et al., Aescin a natural soap for the formation of lipid nanodiscs with tunable size, Soft Matter 17 (2021) 1888–1900.
- [15] R. Geisler, et al., Aescin-induced conversion of gel-phase lipid membranes into bicelle-like lipid nanoparticles, Langmuir 35 (2019) 16244–16255.
- [16] K.D. Tsirigos, et al., Topology of membrane proteins predictions, limitations and variations, Curr. Opin. Struct. Biol. 50 (2018) 9–17.
- [17] S.D. McCalpin, T. Ravula, A. Ramamoorthy, Saponins form nonionic lipid nanodiscs for protein structural studies by nuclear magnetic resonance spectroscopy, J. Phys. Chem. Lett. 13 (2022) 1705–1712.
- [18] W. Lee, M. Tonelli, J.L. Markley, NMRFAM-SPARKY: enhanced software for biomolecular NMR spectroscopy, Bioinformatics 31 (2015) 1325–1327.
- [19] D. Schwarz, et al., Preparative scale expression of membrane proteins in Escherichia coli-based continuous exchange cell-free systems, Nat. Protoc. 2 (2007) 2945–2957
- [20] M. Etzkorn, et al., Cell-free expressed bacteriorhodopsin in different soluble membrane mimetics: Biophysical properties and NMR accessibility, Structure 21 (2013) 394–401.
- [21] R. Geisler, S. Prévost, R. Dattani, T. Hellweg, Effect of cholesterol and ibuprofen on DMPC-β-Aescin Bicelles: a temperature-dependent wide-angle x-ray scattering study, Crystals 10 (2020) 401.
- [22] D. Oesterhelt, W. Stoeckenius, Functions of a new photoreceptor membrane, Proc. Natl. Acad. Sci. USA 70 (1973) 2853–2857.
- [23] A.M. Dummer, et al., Bacterioopsin-Mediated regulation of bacterioruberin biosynthesis in Halobacterium salinarum, J. Bacteriol, 193 (2011) 5658–5667.
- [24] J.K. Lanyi, Bacteriorhodopsin, Annu Rev. Physiol. 66 (2004) 665-688.
- [25] S. Elter, et al., The use of amphipols for NMR structural characterization of 7-TM proteins, J. Membr. Biol. 247 (2014) 957–964.
- [26] V.A. Bjørnestad, R. Lund, Pathways of membrane solubilization: a structural study of model lipid vesicles exposed to classical detergents, Langmuir 39 (2023) 3914–3933.